Electrochimica Acta 469 (2023) 143267

Contents lists available at ScienceDirect

Electrochimica Acta

journal homepage: www.journals.elsevier.com/electrochimica-acta

Functional electrolyte: Design of anti-corrosion additives for Al collectors in LiFSI-based electrolyte

Masaki Deguchi [a,c,*], Yanko Marinov Todorov [b], Koji Abe [a,b]

[a] Graduate School of Sciences and Technology for Innovation, Yamaguchi University, 2-16-1 Tokiwadai, Ube, Yamaguchi 755-8611, Japan
[b] Organization for Research Initiatives, Yamaguchi University, 2-16-1 Tokiwadai, Ube, Yamaguchi 755-8611, Japan
[c] Panasonic Energy Co., Ltd., 1-1 Matsushita-cho, Moriguchi, Osaka 570-8511, Japan

ARTICLE INFO

Keywords:
LIB
Al corrosion
Inhibitor
Wetting additive
Resistance

ABSTRACT

Recent lithium-ion rechargeable batteries (LIBs) are used as large power sources for EVs, etc. Compared to a single cell used in a cellphone, an EV batteries become higher voltage and higher capacity, therefore battery safety became an important issue. To improve the safety of battery, we are focused on increase the flash point of electrolyte. Since the flash point of current electrolytes for EVs is around room temperature, we are working on the development of high-safety electrolytes using solvents with flash points above 100 °C. In this work we used ethylene carbonate (EC) and γ-butyrolactone (GBL) as a high flash point solvent and thermally stable lithium bis (fluorosulfonyl)imide (LiFSI) was used as a Li salt. Since LiFSI corrodes Al current collectors, we report the results of adding a corrosion inhibitor to this high-safety electrolyte.

1. Introduction

Lithium-ion rechargeable batteries (LIBs), which are used in large power supplies such as EVs and Energy Storage System (ESS), have high voltage and capacity by connecting multiple single batteries in series and in parallel, making battery safety an important issue. For this reason, all-solid-state batteries, as well as use of a flame-retardant solid electrolytes, are attracting attention, but they have problems with the battery life and a low-temperature performance. Therefore, expectations for high safety are returning to the liquid-based LIBs.

However, as shown in Table 1, liquid electrolytes consisting of cyclic carbonates such as EC and linear carbonates such as dimethyl carbonate (DMC), ethyl methyl carbonate (EMC), and diethyl carbonate (DEC) have the advantage that the electrolyte has a very low viscosity, but the disadvantage is that the flash point of the electrolyte is too low (about 25 °C for 1 M LiFSI EC/EMC/DMC=3/3/4).

Therefore, research on the flame retardant and nonflammable electrolytes has been active for a long time. Phosphate esters [1–4], halogen-containing compounds [5–8], ionic liquids [9–13], and phosphazenes [14–17], have been considered as flame retardants, but all they still do not reach the level to use in the real battery. Moreover, for nonflammable compounds, even if the battery performance is good, incineration of the waste liquid is difficult, so we must be prepared for a significant increase in disposal costs. Therefore, it must be said, that there is unfortunately no possibility of practical application of these methods. Therefore, we have come up with the idea of using a high flash point solvent. This method is expected to allow incineration of the waste liquid with no deterioration in battery performance.

In this paper, we decided to use cyclic carbonates such as EC and propylene carbonate (PC), and cyclic esters such as GBL as nonaqueous solvents with flash points above 100 °C as high-safety electrolytes. However, such non-aqueous solvents have the disadvantage of not wetting hydrophobic polyolefin separators because of their high polarity.

In 1999, we proposed "functional electrolytes," which are electrolytes with small amounts of additives with a new functions, and have commercialized many additives [18–20]. In this paper, we decided to use n-heptyl pivalate (PV-HP, 1a) and 2-ethylhexyl pivalate (PV-EH, 1b), shown in Fig. 1, which function to improve the permeability of polyolefin separators [21,22]. For the Li salt, we used LiFSI, which has high thermal stability, but it is known to corrode Al current collectors. In this paper, research was conducted to design an electrolyte, that provides both a safety and also inhibits the corrosion of Al current collector. We tested several groups of organic compounds to find a suitable additive to prevent Al corrosion. The compounds used as Al corrosion inhibition additives for Al current collector are shown in Fig. 1 (from 2a to 2 h).

* Corresponding author.
E-mail address: deguchi.masaki@jp.panasonic.com (M. Deguchi).

https://doi.org/10.1016/j.electacta.2023.143267
Received 18 July 2023; Received in revised form 25 September 2023; Accepted 25 September 2023
Available online 26 September 2023

Table 1
Boiling point, melting point, flash point, viscosity, and conductivity of various solvents, wetting additives and electrolytes.

Abbreviation	Name	Boiling point (°C)	Melting point (°C)	Flash point (°C)	Viscosity (mPa s)	Conductivity (25 °C, mS cm^{-1})
Cyclic solvent						
EC	Ethylene carbonate	248	36	152	Solid	–
PC	Propylene carbonate	242	−49	133	2.42	–
GBL	γ-Butyrolactone	204	−43	100	1.75	–
Linear solvent						
DEC	Diethyl carbonate	126	−43	33	0.78	–
EMC	Ethyl methyl carbonate	107	−15	23	0.72	–
DMC	Dimethyl carbonate	90	3	17	0.61	–
Wetting additive						
PV-HP	n-Heptyl pivalate	215 $_{est.}$	N.A.	90	2.02	–
PV-EH	2-Ethylhexyl pivalate	224 $_{est.}$	N.A.	94	2.16	–
Electrolyte (vol/vol/vol)						
1 M LiFSI EC/EMC/DMC=3/3/4		N.A.	N.A.	25	2.66	11.6
1 M LiFSI EC/GBL=3/7		N.A.	N.A.	107	4.51	10.9
1 M LiFSI EC/PC=1/1		N.A.	N.A.	137	6.60	7.42

Wettability improving additives

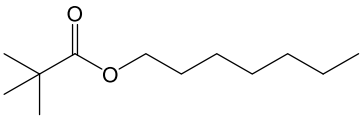

(1a) Heptyl pivalate (PV-HP)

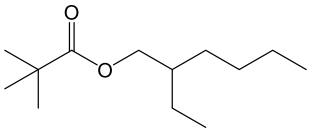

(1b) 2-Ethyl hexyl pivalate (PV-EH)

Al corrosion inhibition additives

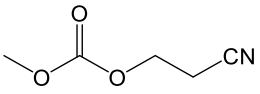

(2a) Cyanoethyl methyl carbonate (CEMC)

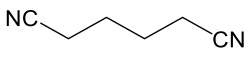

(2b) Adiponitrile (ADN)

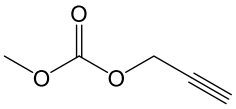

(2c) Propargyl methyl carbonate (PMC)

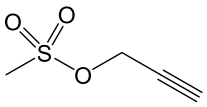

(2d) Propargyl methane sulfonate (PMS)

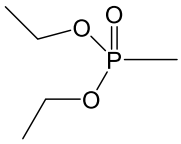

(2e) Diethyl methyl phosphonate (DEMP)

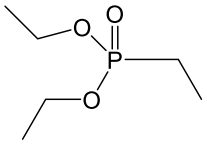

(2f) Diethyl ethyl phosphonate (DEEP)

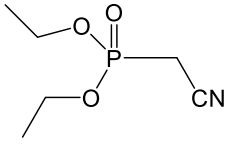

(2g) Diethyl cyanomethyl phosphonate (DECMP)

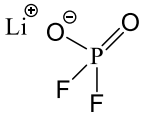

(2h) Lithium difluoro phosphate ($LiPO_2F_2$)

Fig. 1. Structures of the investigated wettability improving additives (1a, 1b), and Al corrosion inhibition additives (from 2a to 2 h).

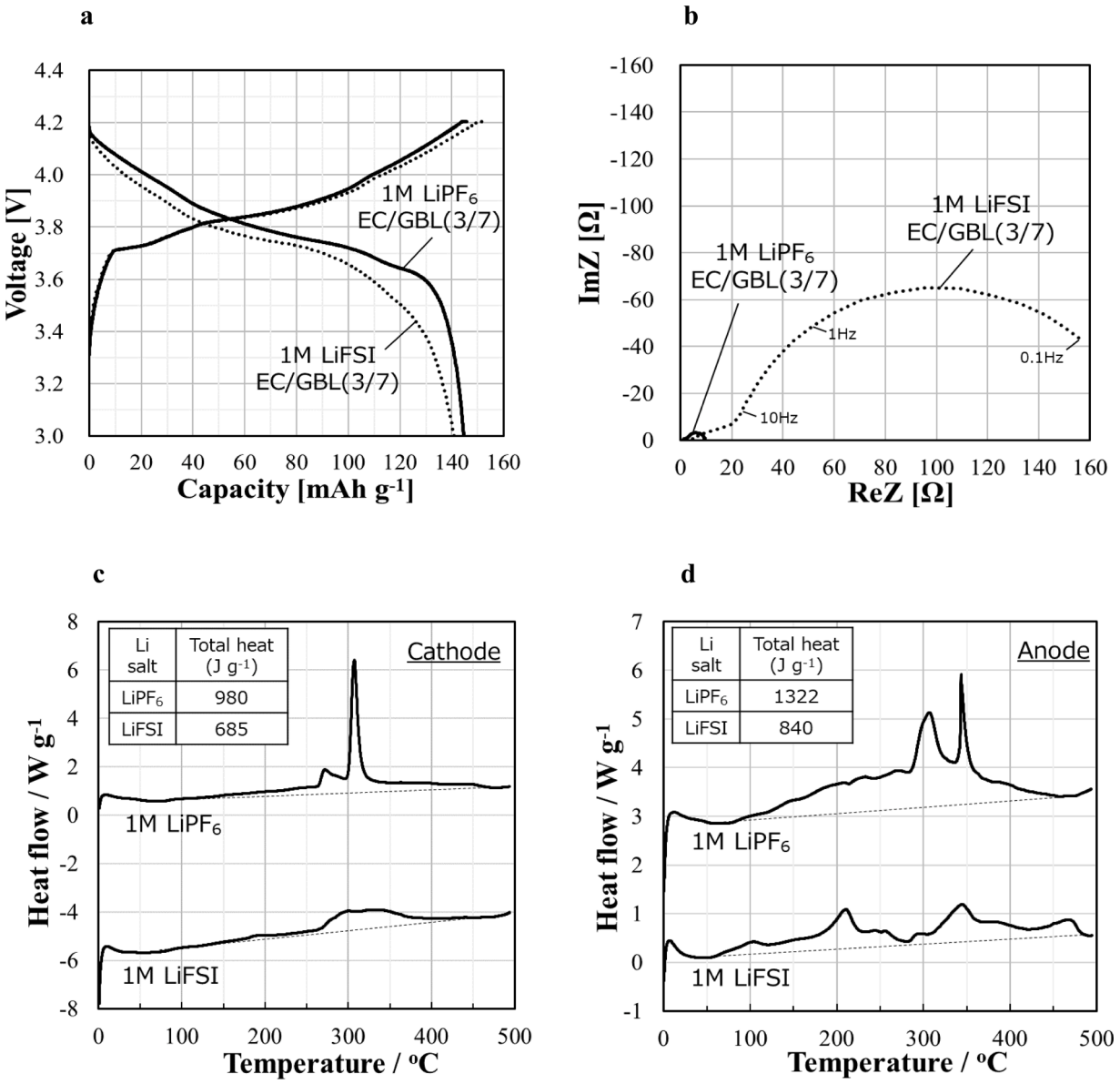

Fig. 2. 2nd cycle charge-discharge curves of the cells with 1 M $LiPF_6$ or 1 M LiFSI in [EC/GBL=3/7(v/v)] +VC(2wt%)+PV-HP(2wt%) (a), Impedance measurement results at 4.2V charged state (2nd cycle charge) (b), and DSC profiles for the cathodes (c) and anodes (d).

2. Experimental

2.1. Chemicals used

The additives to wet the separator, PV-HP(1a) and PV-EH(1b) were both synthesized in our laboratory and doping to the electrolytes was 2wt%. To synthesize PV-HP(1a) 17.0 g (0.165 mol) of pivalic acid and 17.77 g (0.150 mol) of 1-heptanol were added to 1.70 g (0.0165 mol) of 95% sulfuric acid was refluxed for 3 h under Ar. Then, the product was distilled under reduced pressure to yield 28.4 g (Yield, 83.3%) of PV-HP (1a) at 114 °C/3.6 kPa. PV-EH(1b) was also synthesized in the same manner as PV-HP(1a) and distilled at 111 °C/2.9 kPa.

Cyanoethyl methyl carbonate (CEMC, 2a) and propargyl methyl carbonate (PMC, 2c) were also synthesized in our laboratory and addition to the electrolyte was 3wt%. For the synthesis of CEMC(2a), 8.8 g (0.120 mol) of ethylene cyanohydrin, 1.8 g (0.16 mol) of triethylamine, and 40 ml of ethyl acetate (Tokyo Kasei Kogyo Co., Ltd.) were added to a 200 ml three-neck flask. Methyl chloroformate 15.3 g (0.16 mol) was added dropwise under an Ar atmosphere to keep the temperature below 15 °C. After the reaction, triethylamine hydrochloride was removed by washing with H_2O, and the organic layer was dried over $MgSO_4$. Then, the organic layer was distilled under reduced pressure to give 7.1 g (Yield, 93.7%) of CEMC(2a) at 101 °C/0.7 kPa. PMC(2c) was also synthesized in the same manner as CEMC(2a).

Adiponitrile (ADN, 2b), diethyl methyl phosphonate (DEMP, 2e), diethyl ethyl phosphonate (DEEP, 2f), diethyl cyanomethyl phosphonate (DECMP, 2g), lithium difluoro phosphate ($LiPO_2F_2$, 2 h) were purchased from Tokyo Chemical Industry Co. Ltd., and were used without any further purification. Vinylene carbonate (VC) and propargyl methane sulfonate (PMS, 2d) were MU Ionic Solutions Corporation made.

2.2. Solvent and electrolyte property evaluation

Viscosity was measured at 25 °C using BROOK FIELD VISCOMETER DV-I Prime LV.

Electrolyte conductivity was measured by TOADKK ECMETER CM-42X conductivity meter.

To measure the flash point, two types of instruments were used. For

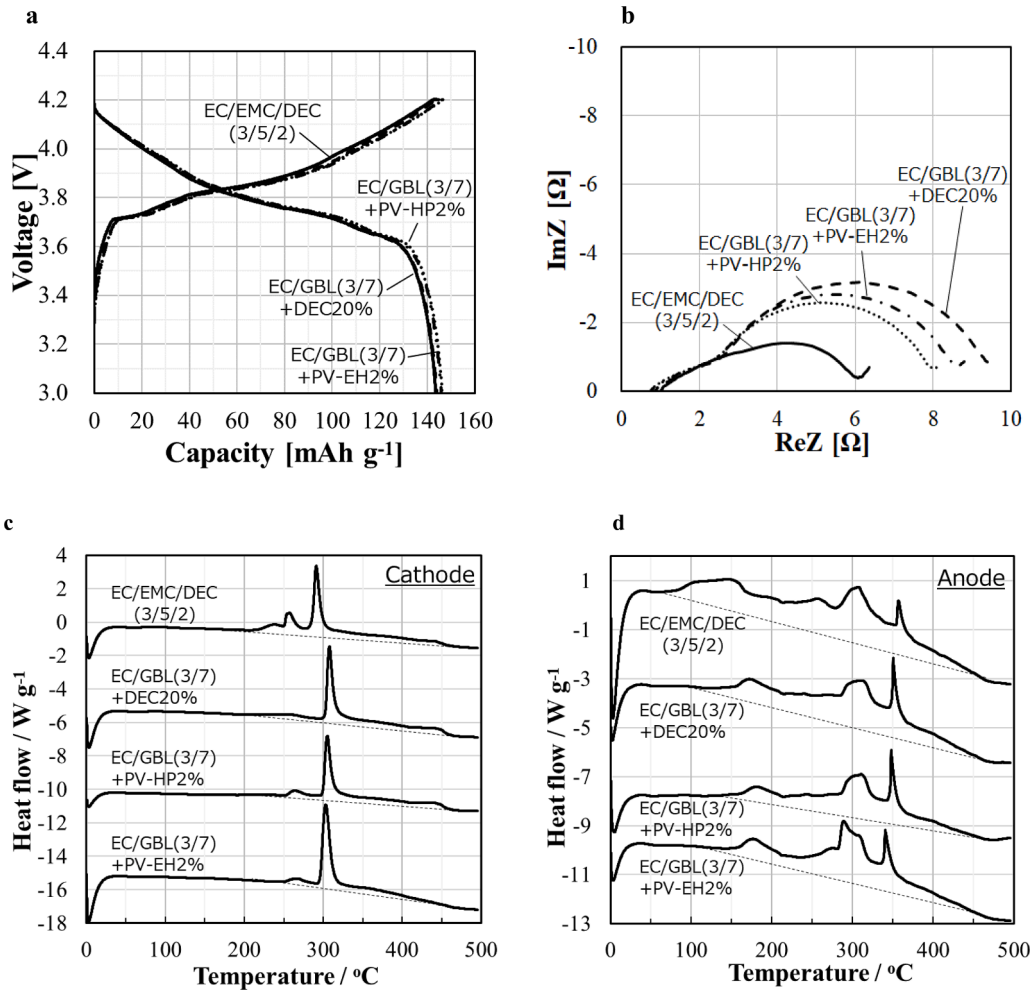

Fig. 3. 2nd cycle charge-discharge curves of the cells with 1 M $LiPF_6$ various solvents (a), Impedance measurement results at 4.2 V charged state (2nd cycle charge) (b), and DSC profiles for the cathodes (c) and anodes (d).

temperatures lower than 90 °C, Tag Flash Point Tester (TAG4, Anton Paar), and for higher flash points, Pensky-martens method (PMA500, Anton Paar) was used.

2.3. Battery performances and impedance evaluation

The laminated cell (14.8 mAh capacity) was used for the evaluation. $LiCoO_2$ from Nichia Corporation was used as the cathode active material, artificial graphite from Resonac Corporation was used as the anode active material, and a polyethylene separator (20 μm thickness) from Asahi Kasei Corporation was used as the separator. The electrolytes used, 1 M $LiPF_6$ [EC/GBL=3/7(v/v)]+VC(2wt%), 1 M LiFSI [EC/GBL=3/7(v/v)]+VC(2wt%), and 1 M $LiPF_6$ [EC/EMC/DEC=3/5/2(v/v/v)]+ VC(2wt%) were MU Ionic Solutions Corporation made.

Battery performances were evaluated using TOSCAT-3100 manufactured by Toyo System Co. Ltd. Charge/discharge evaluation and Al corrosion evaluation were performed at 25 °C, 0.1C rate, 4.1V-cccv / 3.0V-cc for 1st cycle, and 4.2V-cccv / 3.0V-cc for 2nd cycle.

Impedance evaluations were performed using a Solartron 1455A, Solartron, Inc. at 25 °C and 100% SOC (4.2V, 2nd cycle), with a frequency range between 100 KHz and 0.1 Hz.

2.4. Al current collector analysis

The surface of the cathode Al current collector was observed by Scanning Electron Microscope (SEM) and X-ray Photoelectron Spectroscopy (XPS). The sample was prepared by disassembling a discharged laminated battery after 2nd cycle discharge and removing the cathode plate. To remove any residuals of electrolyte, the cathode electrode was washed three times with DMC before SEM and XPS measurements. SEM observations were performed using JEOL's JSM-7001F at a magnification of 200x. XPS measurements were performed using ULVAC-PHI ESCA 5600.

Differential Scanning Calorimetry (DSC, DSC Q1000, TA Instruments Inc.) was used to evaluate the thermal stability of the cathode and anode electrodes. The 2nd cycle charged laminated battery was disassembled, the electrode plates were removed, and the cathode and anode electrodes were each sealed in a measuring pan and heated at 10 °C/min to perform DSC measurements.

3. Results and discussion

3.1. Choice of base electrolyte solvent

As shown in Table 1, the flash point of the EC/GBL or EC/PC based electrolytes was found to be above 100 °C, whereas the flash point of the conventional electrolyte was 25 °C. In addition, the conductivity was found to be higher for EC/GBL than for EC/PC, and the viscosity was found to be lower for EC/GBL than for EC/PC. To obtain a well-balanced electrolyte in terms of conductivity and flash point, in this paper, we decided to use EC/GBL as a non-aqueous solvent composition.

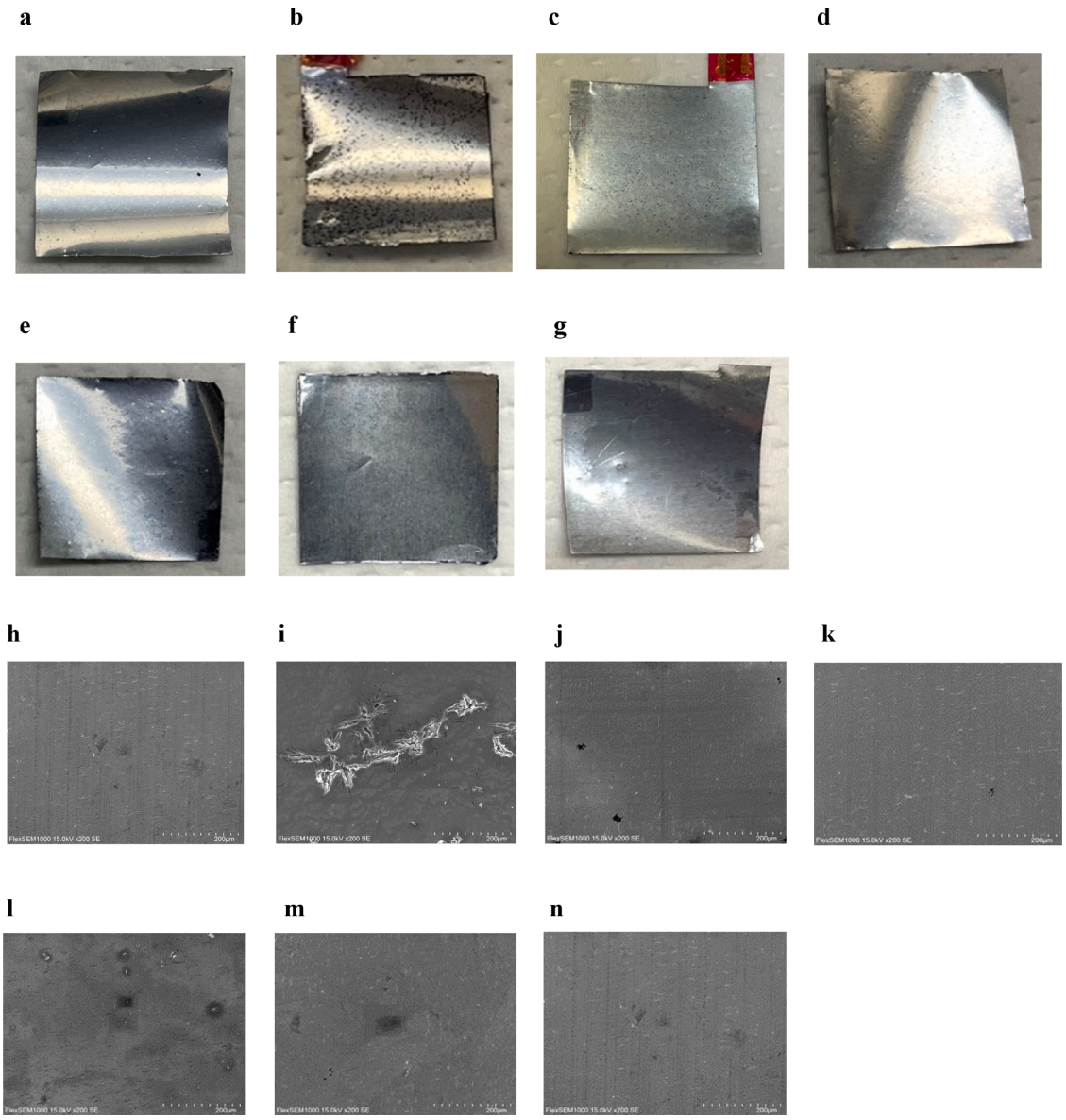

Fig. 4. Photo images (from a to g) and corresponding SEM images (× 200) (from h to n) of Al substrates (back side of cathode) after 2nd cycle discharge. Electrolyte is: 1 M $LiPF_6$ (a, h) or 1 M LiFSI (b, i) in [EC/GBL=3/7(v/v)] +VC(2wt%)+PV-HP(2wt%). Others are 1 M LiFSI (same as b), but +3wt% additives: CEMC (c, j), DECMP (d, k), PMC (e, l), PMS (f, m), and $LiPO_2F_2$ (g, n).

3.2. Choice of Li salt

To decide which Li salt to use, the heat generation of the cathode and anode electrodes using $LiPF_6$ and LiFSI was measured. Pouch cells were prepared using 1 M $LiPF_6$ [EC/GBL=3/7(v/v)]+VC(2wt%)+PV-HP(1a) (2wt%) and 1 M LiFSI [EC/GBL=3/7(v/v)]+VC(2wt%)+PV-HP(1a) (2wt%) as electrolytes. As these electrolytes do not wet the separator, we need to add a wetting additive. To obtain clear results, the wetting additive should be in a small amount. Here PV-HP(1a) was used as a separator wetting additive because only 2wt% is enough to ensure wetting the separator.

2nd cycle charge/discharge curves and impedance measurement results are shown in Fig. 2a and 2b. After charging at 4.2V (2nd cycle), the cell was disassembled, and the cathode and anode electrodes were removed for DSC measurements. As can be seen from Fig. 2c and 2d, the total heat generation at full charge is smaller for LiFSI than for $LiPF_6$. Therefore, we choose LiFSI as a Li salt for this high safety electrolyte.

The above results indicate that the EC/GBL electrolyte has a flash point of 100 °C or higher and that the total heat generated by the cathode and anode electrodes at full charge can be reduced by using LiFSI, which is an advantage in terms of safety.

3.3. Choice of the additives to wet the separator

Next, we investigated the thermal stability of the electrodes in various solvents using $LiPF_6$, which has a characteristic of no Al corrosion, although the total heat generation at full charge in the cathode and anode electrodes is greater than that of LiFSI. Fig. 3c and 3d show the cathode and anode electrodes DSC results at 4.2V state of charge. Compared to the EC/EMC/DEC electrolyte containing 20% DEC, the EC/GBL electrolyte containing 20% DEC was found to suppress heat generation for both the cathode and anode electrodes, especially improving the thermal safety of the anode electrode.

In EC/GBL electrolyte, the separator must contain 20% DEC to wet. On the other hand, EC/GBL electrolyte with PV-HP(1a) and PV-EH(1b) wet the separator even with only 2wt% addition.

Furthermore, as Fig. 3c and 3d show, the EC/GBL electrolyte with PV-HP(1a) and PV-EH(1b) further suppresses the amount of heat

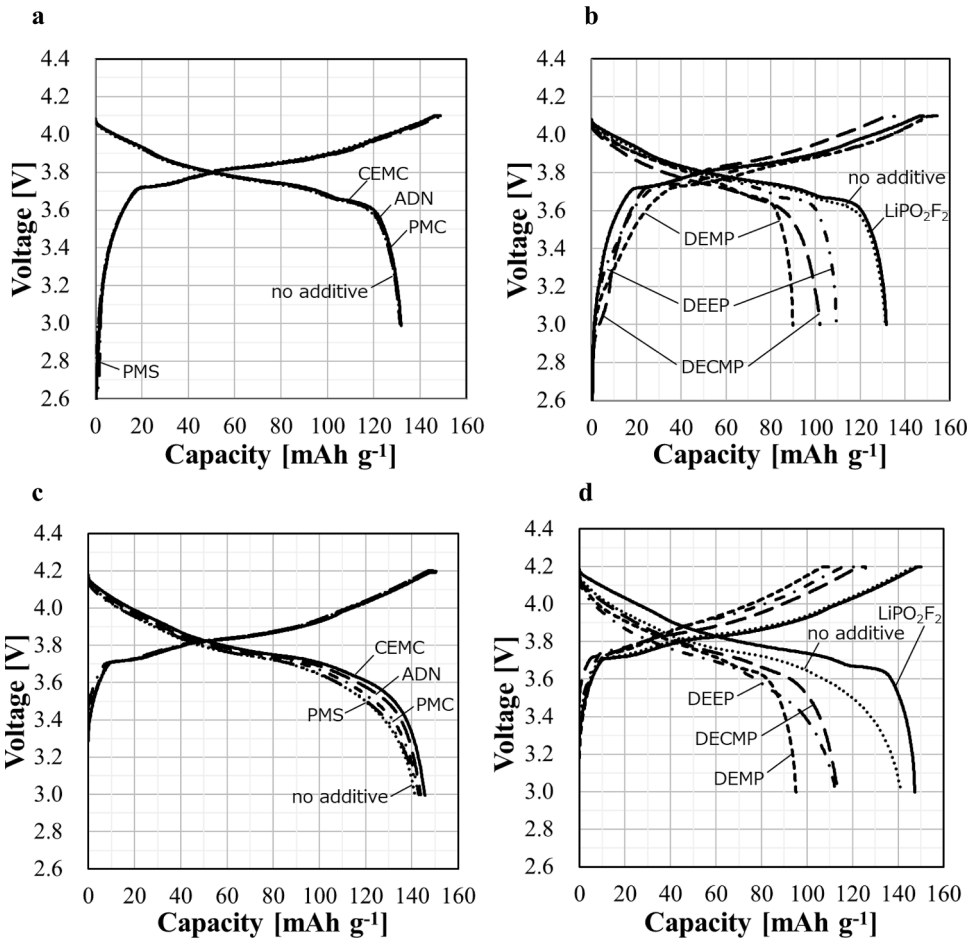

Fig. 5. 1st cycle charge-discharge curves of the cells with -C≡N or -C≡CH triple bond compounds (a) and with organic or inorganic phosphate compounds (b). 2nd cycles are shown in (c) and (d) respectively.

generated in the cathode and anode electrodes. The thermal stability (onset temperature) of both cathode and anode electrodes was improved by about 30 °C compared to the current electrolyte. This improvement may be due to higher flash points of PV-HP(1a) and PV-EH(1b) compared to DMC (Table 1).

The charge/discharge results of the cells with the above electrolytes are shown in Fig. 3a. It was found that the capacities of the electrolytes using EC/GBL were all equivalent to those of the current EC/EMC/DEC based electrolyte. In particular, the electrolyte with the addition of 2wt % PV-HP(1a) or PV-EH(1b), both were found to have slightly improved capacity.

The charge transfer resistance of the cells measured by Electrochemical Impedance Spectroscopy (EIS) using these electrolytes is shown in Fig. 3b. Compared to the EC/GBL electrolyte with 20% DEC, the EC/GBL electrolyte with 2wt% PV-HP(1a) or PV-EH(1b) was found to have a lower cathode impedance on the low frequency side. Therefore, in the subsequent work we decided to use PV-HP(1a) as it had the lowest battery resistance.

3.4. Inhibitors for Al corrosion

Whenever this electrolyte seems to have improved safety, the charge/discharge results shown in Fig. 2a indicate that LiFSI electrolyte causes a capacity decrease during charging and discharging compared to $LiPF_6$ electrolyte. Furthermore, from the impedance results shown in Fig. 2b, it was found that the cathode resistance, observed at low frequency side, increased in the cell using LiFSI electrolyte. Observation of the surface of the Al current collector showed that there were many blackspots on the Al surface of the cathode of the cell with LiFSI electrolyte, as shown in Fig. 4b, and SEM observation (Fig. 4i) revealed that pitting corrosion had occurred.

To suppress this Al corrosion, the compound that prevents corrosion is required. In the LiFSI based electrolyte, Al surface cannot form a strong enough protecting layer like AlF_3 in case of $LiPF_6$. Al corrosion occurs via oxidation of Al current collector surface to produce Al^{3+} during charge of battery. Then Al^{3+} is readily solvated by solvent molecules and therefore dissolves in electrolyte. However, if stronger than solvent ligand is used, then the obtained Al complex compound may stay undissolved at the Al surface and therefore may prevent further corrosion. Another way to prevent the Al corrosion is a simple addition of $LiPF_6$, but according to results above, this may reduce the thermal stability of battery.

In this work, we decided to use organic compounds with -C≡CH or -C≡N groups, as strong ligands are needed to coordinate with Al^{3+}. Phosphate type additives were also tested. All tested compounds are shown in Fig. 1 (from 2a to 2 h). Corrosion inhibition of Al current collector was tested using 1 M LiFSI [EC/GBL=3/7(v/v)]+VC(2wt%)+ PV-HP(1a)(2wt%) as the base electrolyte.

Fig. 5a shows the 1st cycle charge-discharge curves for cyanoethyl methyl carbonate with one -C≡N group (CEMC, 2a), adiponitrile with two -C≡N groups (ADN, 2b), propargyl methyl carbonate with one -C≡CH group (PMC, 2c) and propargyl methane sulfonate (PMS, 2d) with one -C≡CH group. The results of the 2nd cycle charge-discharge curves are shown in Fig. 5c. It was found that all discharge capacities were higher than those without additives. The capacity was higher for CEMC(2a) and ADN(2b) with -C≡N groups, followed by PMC(2c) and

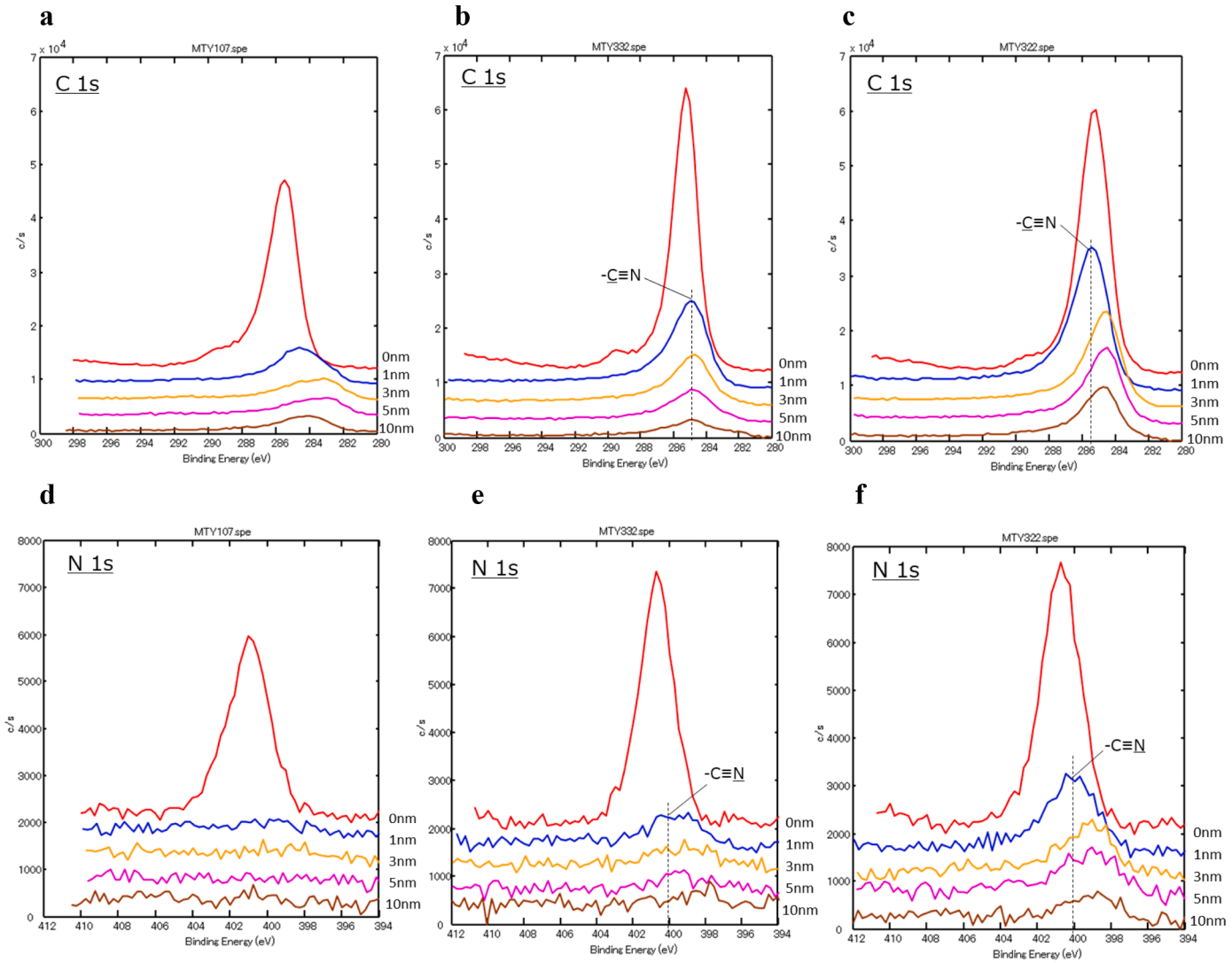

Fig. 6. XPS analysis of Al substrate of the cathodes after 2nd cycle discharge for the cells with: No corrosion inhibitor (a, d), CEMC (b, e), and DECMP (c, f).

PMS(2d) with -C≡CH groups. Next, Fig. 5b shows the 1st cycle charge-discharge curves for the organic phosphate compounds; diethyl methyl phosphonate (DEMP, 2e), diethyl ethyl phosphonate (DEEP, 2f), and diethyl cyanomethyl phosphonate (DECMP, 2g), and for the inorganic phosphate compound; lithium difluoro phosphate ($LiPO_2F_2$, 2 h).

The results of the 2nd cycle charge-discharge curves are shown in Fig. 5d. It was found that DEMP(2e), DEEP(2f), and DECMP(2g) all had a capacity decrease, but only the inorganic $LiPO_2F_2$(2 h) showed very good discharge capacity. Therefore, surface observations of the Al current collectors were performed for CEMC(2a) and DECMP(2g) with -C≡N groups (Fig. 4c and 4d). As a result of visual inspection, the number of blackspots on CEMC(2a) and DECMP(2g) was reduced, and SEM observation also confirmed that pitting corrosion was reduced (Fig. 4j and 4k). In addition, the XPS spectrum is shown in Fig. 6. The peak attributed to -C≡N appeared in the C1s and N1s spectra, indicating that the film containing -C≡N was involved.

Surface observations of the Al current collectors were performed for PMC(2c) and PMS(2d) (Fig. 4e and 4f). The results showed that PMC(2c) and PMS(2d) as well as CEMC(2a) and DECMP(2g) had reduced blackspots on visual inspection. SEM observations also showed that pitting corrosion was also reduced (Fig. 4l and 4m).

Fig. 7d shows the XPS surface analysis of the Al current collector of PMC(2c). The peak of the C1s spectrum at 0 nm in the surface layer increased to 53.0 atom% for PMC(2c), compared to 45.5 atom% without additives (Fig. 7a). The similar trend was observed at a depth of 1 nm, suggesting that the addition of PMC(2c) increase the amount of films containing -C≡CH near the surface layer.

Next, the XPS surface analyses of the Al current collector of PMS(2d) are shown in Fig. 7e, 7f, and 7g. In the S2p spectrum without additives (Fig. 7c), a peak around 171 eV, which seems to be derived from LiFSI, is very strong from 8.9 atom% to 5.5 atom% in the surface layer from 0 nm to 10 nm. In contrast, the peak in the S2p spectrum of the PMS(2d) addition (Fig. 7f) was as high as 6.6 atom% at 0 nm in the surface layer, but disappeared at depths of 1 nm to 10 nm. Furthermore, the N1s spectrum at 0 nm in the surface layer was 3.6 atom% without additives (Fig. 7b), while it was as low as 2.2 atom% with PMS(2d) (Fig. 7e). These results indicate that the addition of PMS(2d) forms some kind of surface protective film and reduces the S and N elements derived from LiFSI. The peak intensity of the C1s spectrum at 0 nm in the surface layer was 45.5 atom% without additives (Fig. 7a), while it was slightly increased to 46.6 atom% with PMS(2d) (Fig. 7g). Hence, it is possible that PMS(2d) like PMC(2c) has an increase in the film containing PMS(2d) derived -C≡CH at the surface layer.

A phenomenon similar to the coordination of -C≡CH groups to the Fe surface in G.W. Poling's paper [23] may be occurring on the Al surface of the cathode. However, this work suggests that compounds containing -C≡N groups have stronger coordination strength to the Al surface than compounds containing -C≡CH groups.

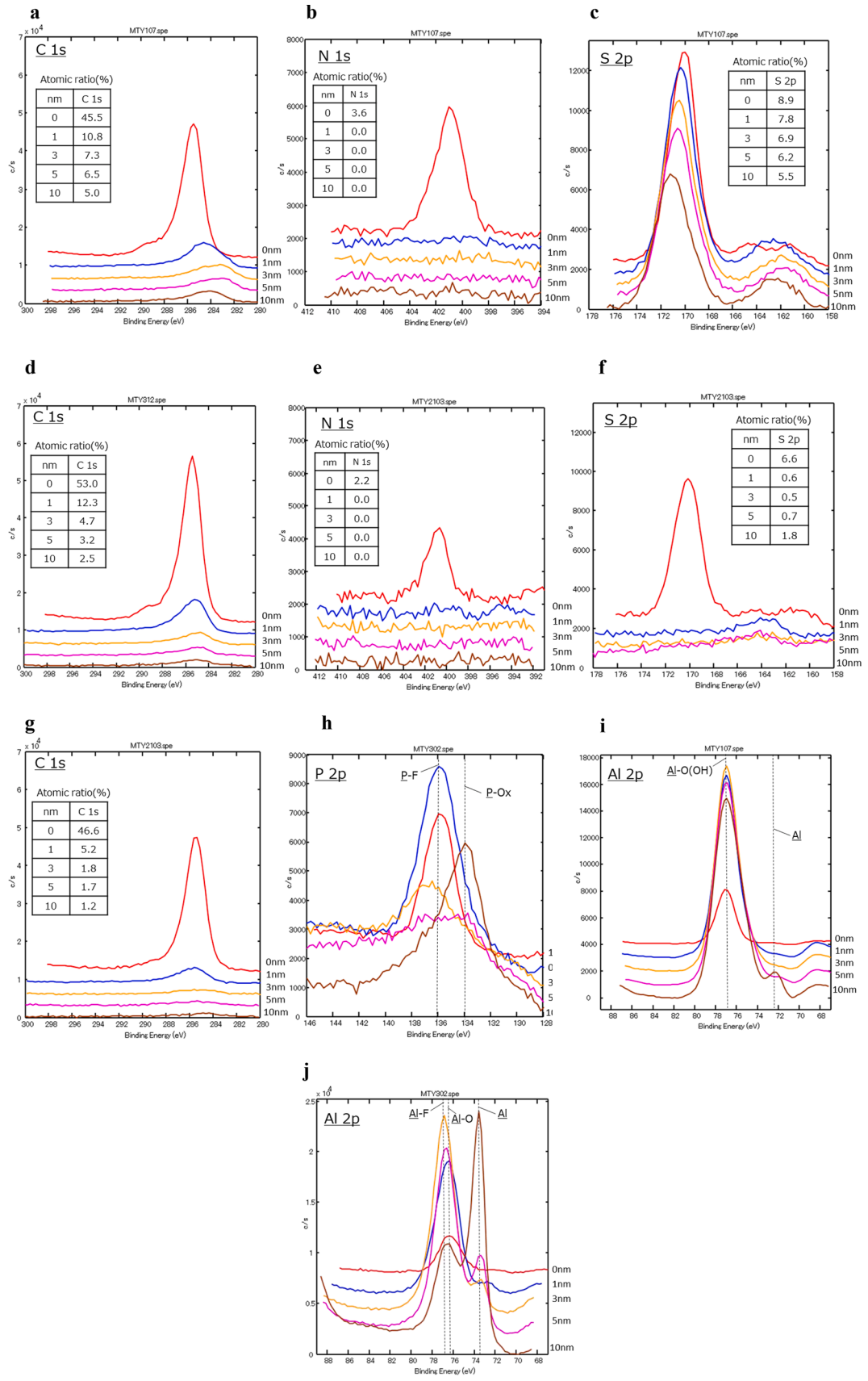

Fig. 7. XPS analysis of Al substrate of the cathodes after 2nd cycle discharge for the cells with: No corrosion inhibitor (a, b, c, i), PMC (d), PMS (e, f, g), and $LiPO_2F_2$ (h, j).

Table 2
Summary of cell performances using electrolytes with Al corrosion inhibition additives.

Cell performances	Organic compounds			Inorganic compound
	Triple bonds With -C≡N groups	With -C≡CH groups	Phosphate With -C≡N groups	Phosphate With Li and F groups
	CEMC(2a), ADN(2b)	PMC(2c), PMS(2d)	DECMP(2g)	$LiPO_2F_2$(2 h)
Capacity at 1st cycle (4.1–3.0 V)	132mAh/g	132mAh/g	109mAh/g	132mAh/g
Capacity at 2nd cycle (4.2–3.0 V)	145mAh/g	142mAh/g	114mAh/g	147mAh/g
Al corrosion behavior (Visual and SEM)	Blackspots and pitting corrosion decrease significantly	Blackspots and pitting corrosion decrease	Blackspots and pitting corrosion decrease	Blackspots and pitting corrosion disappear completely

Visual and SEM results indicate that organic phosphate compounds also have the Al corrosion inhibition effect (Fig. 4). However, since the 2nd cycle discharge capacities of the organic phosphate compounds were all low, the cause of the capacity decrease was not likely due to corrosion (Fig. 5d). In the 1st cycle charge, a shoulder is observed around 3.0 V for all organic phosphate compounds, suggesting that reductive decomposition was occurring on the anode surface (Fig. 5b). For example, DECMP(2g) may be consumed in the 1st cycle charge due to reductive decomposition at the graphite anode interface, resulting in a smaller Al corrosion inhibition effect. In this case, some Li^+ ions were also consumed, which was presumed to reduce the discharge capacity.

The surface observation of the Al current collector of the inorganic phosphate compound ($LiPO_2F_2$, 2 h) shows that the surface condition of $LiPO_2F_2$(2 h) is extremely good, with complete disappearance of blackspots and pitting corrosion (Fig. 4g and 4n). From the XPS analysis of $LiPO_2F_2$(2 h) in Fig. 7h, the presence of a P-F bond peak (136 eV) and a P-O bond peak (134 eV) on the surface of Al in the P2p spectrum suggests that $Al(PO_2F_2)_3$, similar to Al-F, B-O/B-F as in the paper by K. Park et.al. [24] may be formed. Furthermore, in the Al2p spectrum, the Al-O and Al-F bond peaks (76 eV) suggested the presence of films presumed to be Al_2O_3 and AlF_3 (Fig. 7j). On the other hand, in the Al2p spectrum in the absence of $LiPO_2F_2$, an Al-O(OH) peak (77 eV) was observed, and the intensity of the Al metal peak (73 eV) was very small, suggesting Al surface corrosion (Fig. 7i).

Thus, as shown in Table 2, we can conclude that $LiPO_2F_2$(2 h) could form a strong enough protecting layer like $Al(PO_2F_2)_3$ on the Al surface of the cathode and this is the reason for excellent Al corrosion inhibition effect.

4. Conclusion

EC/GBL=3/7(v/v) was found to be a low-viscosity mixed solvent with a flash point above 100 °C and expected to be highly safe. Next, as a Li salt, LiFSI was found to have higher thermal stability of the cathode and anode when fully charged than $LiPF_6$, and even higher safety could be expected. On the other hand, to solve the corrosion of the Al current collector by LiFSI, we investigated the use of triple bond compounds with π-electrons and phosphorus compounds as additives. As a result, it was found that among the triple bond groups, CEMC(2a) and ADN(2b) with -C≡N groups have a greater Al corrosion inhibition effect than PMC(2c) and PMS(2d) with -C≡CH groups.

On the other hand, among the phosphate compounds, the organic phosphate compounds (DEMP(2e), DEEP(2f), and DECMP(2g)) also had Al corrosion inhibition effects, and the organic phosphate compound with -C≡N groups (DECMP, 2g) was found to have the highest Al corrosion inhibition effect. Furthermore, the inorganic phosphate compound ($LiPO_2F_2$, 2 h) was found to be the best additive in terms of both battery performance and corrosion inhibition.

As described above, the high-safety electrolyte with good results in Al corrosion inhibition is expected to greatly improve safety in actual large batteries. We hope that this work will contribute to the development of safer LIBs.

CRediT authorship contribution statement

Masaki Deguchi: Conceptualization, Investigation, Writing – original draft, Writing – review & editing, Visualization. **Yanko Marinov Todorov:** Conceptualization, Investigation, Writing – original draft, Writing – review & editing, Visualization, Supervision. **Koji Abe:** Conceptualization, Investigation, Writing – original draft, Writing – review & editing, Visualization, Supervision.

Declaration of Competing Interest

The authors declare that they have no known competing financial interests or personal relationships that could have appeared to influence the work reported in this paper.

Data availability

The authors do not have permission to share data.

References

[1] X. Wang, E. Yasukawa, S. Kasuya, J. Electrochem. Soc. 148 (10) (2001) A1058, https://doi.org/10.1149/1.1397773.
[2] H.Y. Xu, S. Xie, Q.Y. Wang, X.L. Yao, Q.S. Wang, C.H. Chen, Electrochim. Acta 52 (2) (2006) 636–642, https://doi.org/10.1016/j.electacta.2006.05.043.
[3] Y.M. Todorov, K. Fujii, N. Yoshimoto, D. Hirayama, M. Aoki, H. Miura, M. Morita, Phys. Chem. Chem. Phys. 46 (2017), https://doi.org/10.1039/c7cp06438a.
[4] Y.M. Todorov, M. Aoki, H. Miura, K. Fujii, N. Yoshimoto, M. Morita, J. Power Sources 332 (2016) 322, https://doi.org/10.1016/j.jpowsour.2016.09.119.
[5] K. Xu, M. Ding, S. Zhang, J. Allen, T.R. Jow, J. Electrochem. Soc. 149 (8) (2002) A1079–A1082, https://doi.org/10.1149/1.1490356.
[6] M. Morita, T. Kawasaki, N. Yoshimoto, M. Ishikawa, Electrochemistry 71 (12) (2003) 1067–1069, https://doi.org/10.5796/electrochemistry.71.1067.
[7] M. Ihara, B.T. Hang, K. Sato, M. Egashira, S. Okada, and J. Yamaki, J. Electrochem. Soc., 150, A1476–A1483. doi:10.1149/1.1614269.
[8] T. Dagger, C. Lürenbaum, F.M. Schappacher, M. Winter, J. Power. Sources 342 (2017) 266–272, https://doi.org/10.1016/j.jpowsour.2016.12.007.
[9] A. Chagnes, M. Diaw, B. Carré, P. Willmann, D. Lemordant, J. Power Sources 145 (2005) 82–88, https://doi.org/10.1016/j.jpowsour.2004.12.035.
[10] H. Nakagawa, Y. Fujino, S. Kozono, Y. Katayama, T. Nukuda, H. Sakaebe, H. Matsumoto, K. Tatsumi, J. Power Sources 174 (2007) 1021–1026, https://doi.org/10.1016/j.jpowsour.2007.06.133.
[11] M. Watanabe, M.L. Thomas, S. Zhang, K. Ueno, T. Yasuda, K. Dokko, Chem. Rev. 117 (2017) 7190–7239, https://doi.org/10.1021/acs.chemrev.6b00504.
[12] D. Ding, Y. Maeyoshi, M. Kubota, J. Wakasugi, K. Kanamura, H. Abe, J.Power. Sources 506 (2021), 230099, https://doi.org/10.1016/j.jpowsour.2021.230099.
[13] H.T. Kim, J. Kang, J. Mun, S.M. Oh, T. Yim, Y.G. Kim, ACS Sustain. Chem. Eng. 4 (2016) 497–505, https://doi.org/10.1021/acssuschemeng.5b00981.
[14] C.W. Lee, R. Venkatachalapathy, J. Prakash, Electrochem. Solid-State Lett. 3 (2) (2000) 63, https://doi.org/10.1149/1.1390959.
[15] M. Otsuki, T. Ogino, K. Amine, ECS Trans. 1 (24) (2006) 13–19, https://doi.org/10.1149/1.2209348.
[16] T. Tsujikawa, K. Yabuta, T. Matsushita, T. Matsushima, K. Hayashi, M. Arakawa, J. Power.Sources 189 (2009) 429, https://doi.org/10.1016/j.jpowsour.2009.02.010.
[17] L. Du, X. Hou, W. Zhao, L. Haneke, J. Wang, X. Ju, X. Liu, Y. Yang, J. M. Wrogemann, S. Künne, Martin Winter, T. Placke, J. Li, J.Power.Sources 541 (2022), 231670, https://doi.org/10.1016/j.jpowsour.2022.231670.
[18] K. Abe, T. Hattori, K. Kawabe, Y. Ushigoe, H. Yoshitake, J. Electrochem. Soc. 154 (2007) A810, https://doi.org/10.1149/1.2746570.
[19] K. Abe, T.Hattori K.Miyoshi, Y. Ushigoe, H. Yoshitake, J. Power Sources 184 (2008) 449, https://doi.org/10.1016/j.jpowsour.2008.03.037.
[20] K. Abe, M. Colera, K. Shimamoto, M. Kondo, K. Miyoshi, J. Electrochem. Soc. 161 (2014) A863, https://doi.org/10.1149/2.086405jes.
[21] D. Tazoe, Y.M. Todorov, K. Abe, in: Fall Meeting, The Electrochemical Society of Japan, 2021, p. 2G01.

[22] M. Deguchi, Y.M. Todorov, K. Abe, in: The 64th Battery Symposium in Japan, 2023, p. 3A18.
[23] G.W. Poling, J. Electrochem. Soc. 114 (1967) 1209, https://doi.org/10.1149/1.2426451.
[24] K. Park, S. Yu, C. Lee, H. Lee, J. Power Sources 296 (2015) 197–203, https://doi.org/10.1016/j.jpowsour.2015.07.052.